Polyhedron 289 (2026) 118009

Contents lists available at ScienceDirect

Polyhedron

journal homepage: www.elsevier.com/locate/poly

A new 3D Ba(II) coordination polymer based on 3-(3-carboxyphenyl)-isonicotinic acid: structural studies and its catalytic role in benzylic alcohol oxidation

Tai Xi-Shi [a,*], Wang Li-Hua [b], Saud I. Al-Resayes [c], Mohammad Azam [c,*]

[a] College of Chemistry and Chemical Engineering, Weifang University, Weifang 261061, PR China
[b] College of Biology and Oceanography, Weifang University, Weifang 261061, PR China
[c] Department of Chemistry, College of Science, King Saud University, P.O. Box 2455, Riyadh 11451, Saudi Arabia

ARTICLE INFO

Keywords:
Ba(II) coordination polymer
Structural characterization
DFT calculation
Catalytic activity

ABSTRACT

A novel 3D Ba(II) coordination polymer derived from 3-(3-carboxyphenyl)isonicotinic acid (H_2L), abbreviated as $[Ba(\mathbf{L})(H_2O)_3]_n$, was synthesized *via* a one-pot reaction in an ethanol/H_2O/DMF mixture (v/v/v = 4:2:1). The composition and purity of the polymer were confirmed using elemental analysis (EA), IR spectroscopy, UV/vis spectroscopy, powder X-ray diffraction (PXRD), and thermogravimetric analysis (TGA). Single-crystal X-ray diffraction revealed that the complex crystallizes in the monoclinic system with space group $P_12_1/c1$, revealing that the Ba(II) center is nine-coordinated, with four oxygen atoms from three individual L ligands, one nitrogen atom from a single L ligand, and four oxygen atoms from coordinated water molecules. The HOMO-LUMO orbital distribution indicates an energy gap of 0.080972 Ha (2.441 eV). The electrostatic potential shows that regions of higher potential are mainly concentrated in the six-membered aromatic rings, while lower-potential regions are found near oxygen and nitrogen donor atoms. Furthermore, the Ba(II) coordination polymer exhibits promising catalytic activity, achieving a 66.3% conversion of benzyl alcohol and a 46.4% yield of benzaldehyde under 5 bar O_2 for a duration 2 h in THF.

1. Introduction

Coordination polymers (CPs) are typically constructed from metal ions bridged by multidentate organic ligands, forming diverse one-dimensional to three-dimensional architectures with tunable structural and physicochemical properties [1–10]. Their interesting topologies and functional versatility make them attractive for gas storage, purification, catalysis, biomedicine, fluorescence sensing, magnetism, pollutant removal, drug delivery, molecular recognition, and illicit drug detection [1–10]. However, selecting metal ions, organic linkers, and reaction conditions, such as temperature and pH, enables precise modulation of CP topology and functionality [11,12]. These materials are beneficial for adsorption, selective catalytic conversions, and biomedical applications due to their high porosity, structural flexibility, and numerous functional sites [4,13–16]. Over recent decades, significant advances in the development of metal–organic frameworks (MOFs) have enabled precise control over their size, shape, and functionality. Solvothermal [17] and hydrothermal [18] methods are still widely used to produce highly crystalline materials. Nevertheless, rising demands for sustainability, cost efficiency, and scalability have led to the development of alternative methodologies, including sonochemical and electrochemical methods [19], microwave-assisted synthesis [20], the UARM process [21], and precipitation-based strategies [22], each offering distinct benefits for the customization of MOF structures.

Although alkaline-earth (AE) metals have significant potential for constructing coordination polymers (CPs), their use in this area remains relatively limited, mainly due to the variable and highly flexible coordination environments of AE ions, which complicate the rational design of specific structures [23]. However, this adaptability also opens the door to the development of unique and diverse structural motifs. Additionally, the large ionic radii of AE metals and their strong affinity for oxo groups make them well-suited for forming robust CP frameworks from multifunctional carboxylate linkers [23]. Among different alkaline-earth metal centers, barium(II) ions have emerged as promising nodes in constructing coordination polymers, despite being less studied than transition- or lanthanide-metal centers [24–29]. Barium, with its

* Corresponding authors.
E-mail addresses: taixs@wfu.edu.cn (T. Xi-Shi), mhashim@ksu.edu.sa (M. Azam).

https://doi.org/10.1016/j.poly.2026.118009
Received 27 November 2025; Accepted 30 January 2026
Available online 4 February 2026

large ionic radius, high coordination number (typically 8–12), and flexible coordination geometry, serves as an excellent building block for the construction of intricate coordination polymers with main-group metals. These structural features facilitate the formation of extended frameworks with accessible metal sites, thereby enhancing overall structural stability and providing active centers suitable for catalytic uses. Catalytic oxidation of benzyl alcohol to benzaldehyde is of particular interest due to the industrial importance of benzaldehyde as a key intermediate. Traditional methods typically depend on stoichiometric amounts of toxic oxidants, peroxides, and halides [30,31], raising environmental and handling concerns. In this context, developing efficient, selective, and environmentally friendly catalytic systems has become a key focus in green chemistry. Heterogeneous catalysts, especially coordination polymers, are very attractive because they provide significant advantages, such as easy separation from reaction mixtures, recyclability, and the ability to incorporate specific active sites within a stable structure framework [32].

In continuation of our previous work on the structural and functional properties of metal complexes formed from carboxylate ligands [33–37], herein we report the synthesis of a novel 3D Ba(II) coordination polymer, $[Ba(L)(H_2O)_3]_n$, [H_2L = 3-(3-carboxy-phenyl)-isonicotinic acid. The complex was obtained *via* a one-pot reaction using a solvent mixture of ethanol, H_2O, and DMF in a 4:2:1 (v/v/v) ratio. Its composition and purity were determined through elemental analysis, infrared spectroscopy (IR), UV–vis spectroscopy, powder X-ray diffraction (PXRD), and thermogravimetric analysis (TGA). The crystal structure was determined using single-crystal X-ray diffraction, providing detailed insight into the coordination environment of the Ba(II) center (Fig. 1). To elucidate further the electronic properties of the polymer, the HOMO–LUMO distribution and electrostatic potential surface were calculated, providing additional insight into its bonding characteristics and potential reactivity. Catalytic investigations revealed that the Ba(II) coordination polymer exhibits significant activity in the oxidation of benzyl alcohol, achieving 66.3% conversion and a 46.4% yield of benzaldehyde under 5 bar O_2 for 2 h in THF.

2. Experimental

2.1. Materials and measurements

All the chemical reagents of 3-(3-carboxy-phenyl)-isonicotinic acid (H_2L), NaOH, $BaCl_2$, ethanol, and DMF used in the experiment are of analytical purity. C, H, and N were measured using an Elementar Vario III EL elemental analyzer (Elementar, Germany). UV–vis spectra were carried out with a PERSEE T9 spectrophotometer (Beijing, China). The IR spectra were measured using an FTIR-850 spectrophotometer (Tianjin Gangdong). PXRD was analyzed on a XD-3 powder diffractometer (Beijing, China). TG-DTA was carried out on a HENVEN HCT-2 thermal analyzer (Beijing, China). Single-crystal data for the Ba(II) coordination polymer were collected on a Bruker Smart CCD diffractometer (Bruker, Billerica, MA, USA). The conversion of benzyl alcohol and the yield of benzaldehyde were analyzed using a GC-6890 gas chromatograph (Purkinje General Instrument Co., Ltd., China) equipped with an SE-54 capillary column (30 m × 0.25 mm × 0.25 μm).

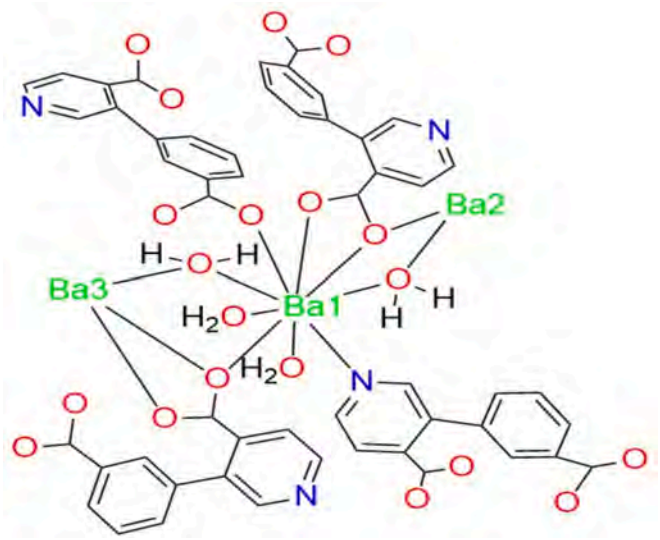

Fig. 1. The coordination mode of Ba(II).

2.2. Synthesis of Ba(II) coordination polymer, $[Ba(L)(H_2O)_3]_n$

0.0607 g (0.25 mmol) of 3-(3-carboxy-phenyl)-isonicotinic acid and 0.020 g (0.5 mmol) of NaOH were added to a 20 mL solution of ethanol/H_2O/DMF (v:v:v = 4:2:1). Barium chloride (0.0521 g, 0.25 mmol) was then added, and the reaction mixture was heated at 85 °C with stirring for six hours. Subsequently, the mixture was cooled to room temperature and stirred for an additional two hours before filtration. Colorless crystals of $[Ba(L)(H_2O)_3]_n$ were formed after 18 days of slow crystallization.

Anal. Calcd. For $[Ba(L)(H_2O)_3]_n$: C, 36.06; H, 3.01; N, 3.24%. Found: C, 35.79; H, 3.39; N, 3.01%.

2.3. Crystal structure determination

The block crystal of Ba(II) coordination polymer with approximate dimensions of 0.13 mm × 0.11 mm × 0.09 mm was selected for single-crystal X-ray diffraction data collection on a Bruker Smar CCD area detector equipped with graphite-monochromated Mo Kα radiation (λ = 0.71073 Å) at 293 K. The structure was solved by the direct method using SHELXT 2014/5 [38] and refined by full-matrix least-squares on F^2 using SHELXL 2018/3 [39]. All non-hydrogen atoms were refined anisotropically and hydrogen atoms were determined with theoretical calculations. The key crystallographic data for the Ba(II) coordination polymer are summarized in Table 1.

2.4. General procedure for the oxidation of benzyl alcohol

The selective oxidation of benzyl alcohol was carried out in a 10 mL

Table 1
The key crystallographic data for the Ba(II) coordination polymer.

Empirical formula	$C_{13}H_{13}NO_7Ba$
Formula weight	432.58
Temperature/K	293
Crystal size/mm^3	0.13 × 0.11 × 0.09
Crystal system	Monoclinic
Space group	$P2_1/c$
a/Å	12.712(4)
b/Å	12.526(3)
c/Å	9.182(2)
β/°	100.036(11)
Volume/Å^3	1439.7(7)
Z	4
ρ_{calc}, mg/mm^3	1.996
S	1.067
$F(000)$	840
Index ranges	$-16 \le h \le 16$, $-16 \le k \le 16$, $-11 \le l \le 11$
Reflections collected	17,558
Independent reflections	3047[R(int) = 0.0688]
Data/restraints/parameters	3047/0/201
Goodness-of-fit on F^2	1.067
Refinement method	Full-matrix least-squares on F^2
Final R indexes [$I \ge 2\sigma(I)$]	R_1 = 0.0340, wR_2 = 0.0865
Final R indexes [all data]	R_1 = 0.0368, wR_2 = 0.0895

stainless steel high-pressure reactor at 5 bar of O_2. A typical reaction mixture contained 20 mg of Ba(II) coordination polymer catalyst, 1 mmol of benzyl alcohol, and 7 mL of tetrahydrofuran (THF). Before heating, the reactor was purged three times with pure O_2 to ensure an oxygen-rich atmosphere, and the pressure was maintained at 5 bar O_2. The reaction was conducted at 80 °C for 2 h under vigorous stirring (2000 rpm) using a heated magnetic stirrer. After completion, the Ba(II) coordination polymer catalyst was recovered by centrifugation (13,000 ×*g*, 10 min), washed three times with ethanol, and dried at 80 °C for reuse.

3. Results and discussion

3.1. Infrared spectroscopy

The infrared spectra of 3-(3-carboxy-phenyl)-isonicotinic acid and Ba(II) coordination polymer are shown in Fig. 2. The free ligand, 3-(3-carboxy-phenyl)-isonicotinic acid, exhibits characteristic absorption peaks of C═O band of carboxylic acid group at *ca.* 1701 cm^{-1}, and the C—N of pyridine ring at *ca.* 1320 cm^{-1} [40]. However, in the Ba(II) coordination polymer, these bands shift to *ca.* 1572 cm^{-1} and 1255 cm^{-1}, respectively, indicating coordination of the carboxylate O atoms and the pyridine N atom to the Ba(II) center.

3.2. UV–Vis spectra

The UV–vis spectra of the free ligand, 3-(3-carboxy-phenyl)-isonicotinic acid, and the Ba(II) coordination polymer with a concentration of 1.0×10^{-4} mol/L in aqueous solution are shown in Fig. 3. The free ligand exhibits two absorption bands at 192 and 220 nm, attributed to π–π^* transition. The Ba(II) coordination polymer exhibits a single absorption band at 196 nm (π–π^*), which is redshifted relative to the ligand, indicating its coordination to the Ba(II) ion. Additionally, to assess the structural stability of the recycled catalyst after the catalytic reaction, the UV-vis spectrum of the recycled Ba(II) coordination polymer at the same concentration was also recorded (Fig. 3), exhibiting a single band at 197 (π–π^*), indicating that the Ba(II) coordination polymer catalyst retains its structural integrity after the catalytic reaction.

3.3. Thermogravimetric analysis

The thermogravimetric analysis (TGA) of the Ba(II) coordination polymer was conducted in an air atmosphere over a temperature range of 25–600 °C with a controlled heating rate of 10 °C min^{-1} (Fig. 4). The

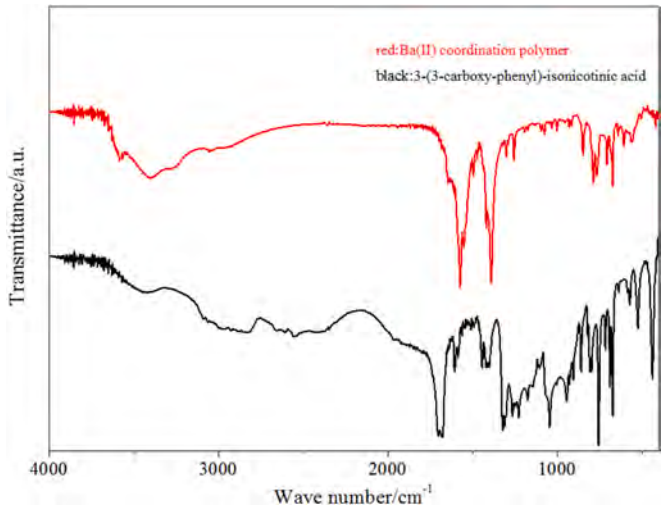

Fig. 2. IR spectra of 3-(3-carboxy-phenyl)-isonicotinic acid and Ba(II) coordination polymer.

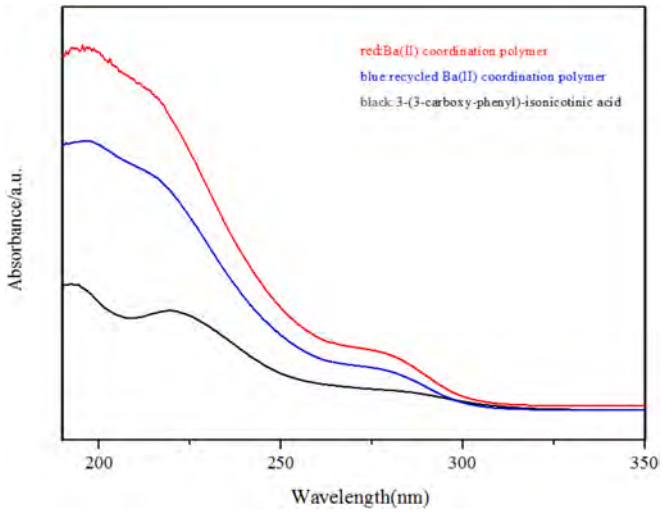

Fig. 3. UV–Vis spectra of 3-(3-carboxy-phenyl)-isonicotinic acid, Ba(II) coordination polymer, and the recycled Ba(II) coordination polymer.

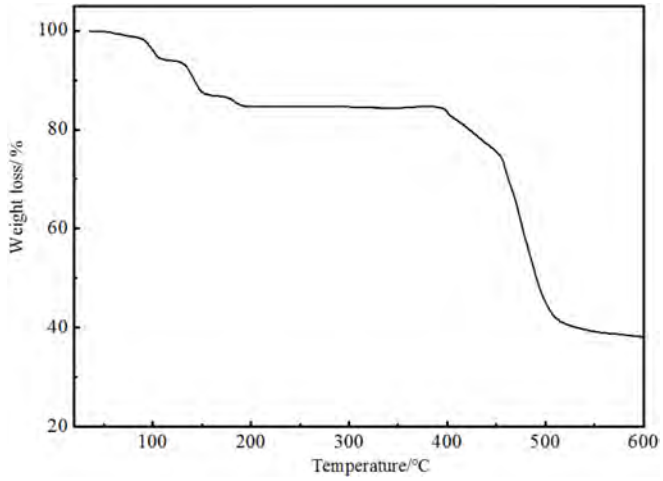

Fig. 4. Thermal stability curve of the Ba(II) coordination polymer.

TGA profile shows three distinct stages of mass loss. The first stage, occurring between 25 and 105 °C, shows a mass loss of approximately 5.8%, which is attributed to the release of adsorbed water molecules. The absence of significant structural decomposition in this temperature range confirms that the framework remains intact during moisture loss. The second stage, observed in the 105–200 °C range, corresponds to a mass loss of about 14.8% (calcd. 12.48%), consistent with the removal of three coordinated water molecules. The good agreement between the experimental and calculated mass-loss values supports the proposed coordination environment and confirms the presence of three bound water molecules in the structure. The third and major decomposition step begins above 395 °C, resulting in a substantial mass loss of approximately 62.2% (calcd. 64.6%) by 600 °C. This significant reduction indicates the decomposition of the organic ligand framework and the collapse of the coordination polymer structure. The final residue at 600 °C is identified as BaO, indicating complete decomposition of the organic framework at high temperatures. Overall, the TGA measurements corroborate the presence of both adsorbed and coordinated water in the Ba(II) coordination polymer and demonstrate thermal stability up to approximately 395 °C, after which structural deterioration occurs.

3.4. Structural description of Ba(II) coordination polymer

The molecular structure of the Ba(II) coordination polymer is shown in Fig. 5, with the selected bond lengths and bond angles summarized in Table 2. The coordination modes of the COO^- groups are shown in Fig. 6. The three-dimensional supramolecular network formed through π–π interactions is illustrated in Fig. 7. As shown in Fig. 5, each Ba(II) center is coordinated by one deprotonated 3-(3-carboxy-phenyl)-isonicotinic acid ligand and three water molecules, resulting in a nine-coordinate environment. The Ba(II) ion adopts a distorted mono-capped square antiprism geometry, coordinated by four oxygen atoms (O1, O4, O7, and $O7^4$) from three COO^- groups belonging to three different deprotonated 3-(3-carboxy-phenyl)-isonicotinic acid ligands, one nitrogen atom (N1) from the isonicotinate moiety, and four oxygen atoms (O3, O5, O6, and $O6^3$) from four coordinated water molecules. The carboxylate groups in the Ba(II) coordination polymer exhibit two different coordination modes (Fig. 6). The carboxylate group attached to the pyridine ring functions in a tridentate fashion, whereas the carboxylate group attached to the benzene ring displays a monodentate coordination mode (Fig. 6). The Ba—O and Ba—N bond distances are within expected ranges for Ba(II) coordination polymers. The Ba—O and Ba—N bond lengths are 2.753(3) Å (Ba1-O1), 2.758(2) Å (Ba1-O4), 3.042(3) Å (Ba1-$O6^3$), 2.817(3) Å (Ba1-O6), 2.695(3) Å (Ba1-O7), 3.137 (3) Å (Ba1-$O7^4$), 2.797(2) Å (Ba1-O5), 2.923(3) Å (Ba1-O3), and 2.950 (2) Å (Ba1-N1), respectively. The O-Ba-O bond angles around Ba(II) vary from 43.07(8)° (O1-Ba1-$O7^4$) to 155.93(8)° ($O7^4$-Ba1-O5), and the O-Ba-N bond angles vary from 70.11(8)° (O3-Ba1-N1) to 156.29(8)° (O4-Ba1-N1). These values align with those of similar barium coordination polymers reported in the literature [41,42]. These varied coordination modes, along with the metal–ligand connectivity, play a crucial role in building the extended polymeric structure. Furthermore, π–π stacking interactions between the aromatic rings provide additional stabilization to the three-dimensional supramolecular framework (Fig. 7). In this structure, the deprotonated 3-(3-carboxy-phenyl)-isonicotinic acid ligands, along with the bridging coordinated water molecules, connect adjacent Ba(II) ions to generate a three-dimensional network structure (Fig. 7).

3.5. DFT calculations of the Ba(II) coordination polymer

The molecular electrostatic potential and orbital simulations of the Ba(II) coordination polymer were performed using the DMol3 module in Materials Studio 2020, with the generalized gradient approximation

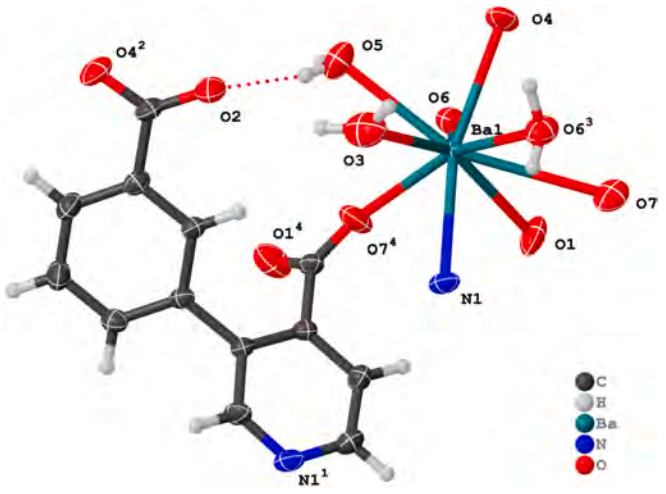

Fig. 5. The molecular structure of Ba(II) coordination polymer (symmetry operation: 1: 2-*x*,1-*y*, 2-*z*; 2: 1-*x*, −1/2 + *y*, 3/2-*z*; 3: +*x*, 3/2-*y*, 1/2 + *z*; 4: +*x*, 3/2-*y*, −1/2 + *z*).

Table 2
Selected bond lengths and angles of Ba(II) coordination polymer.

Bond	*d*	Angle	(°)
Ba1-O1	2.753(3)	O1-Ba1-O4	102.15(9)
Ba1-O4	2.758(2)	O1-Ba1-$O6^3$	62.24(8)
Ba1-$O6^3$	3.042(3)	O1-Ba1-O6	102.47(8)
Ba1-O6	2.817(3)	O1-Ba1-$O7^4$	43.07(8)
Ba1-O7	2.695(3)	O5-Ba1-O1	138.43(8)
Ba1-O5	2.797(2)	O1-Ba1-N1	81.13(9)
Ba1-N1	2.950(2)	O3-Ba1-O1	151.21(9)
Ba1-O3	2.923(3)	O4-Ba1-$O6^3$	66.73(8)
Ba1-$O7^4$	3.137(3)	O6-Ba1-O4	81.57(8)
		$O7^4$-Ba1-O4	84.64(8)
		O4-Ba1-O5	71.48(8)
		O4-Ba1-N1	156.29(8)
		O3-Ba1-O4	104.69(9)
		O6-Ba1-$O6^3$	138.97(6)
		$O7^4$-Ba1-O6	61.04(7)
		$O7^4$-Ba1-$O6^3$	89.62(7)
		O6-Ba1-N1	74.82(8)
		O6-Ba1-O3	71.70(9)
		O7-Ba1-O1	77.42(9)
		O7-Ba1-O4	123.26(8)
		O7b-Ba1-O6	154.91(8)
		O7-Ba1-$O6^3$	63.56(7)
		O7-Ba1-$O7^4$	119.81(9)
		O7-Ba1-O5	73.36(9)
		O7-Ba1-N1	80.45(8)
		O7-Ba1-O3	96.12(9)
		O5-Ba1-$O6^3$	78.37(7)
		O5-Ba1-O6	116.47(8)
		$O7^4$-Ba1-O5	155.93(8)
		O5-Ba1-N1	121.38(8)
		O5-Ba1-O3	62.03(8)
		$O6^3$-Ba1-N1	132.44(7)
		$O7^4$-Ba1-N1	82.06(8)
		O3-Ba1-$O6^3$	139.67(9)
		$O7^4$-Ba1-O3	129.93(9)
		O3-Ba1-N1	70.11(8)

Symmetry operation: 3: +*x*, 3/2-*y*, 1/2 + *z*; 4: +*x*, 3/2-*y*, −1/2 + *z*.

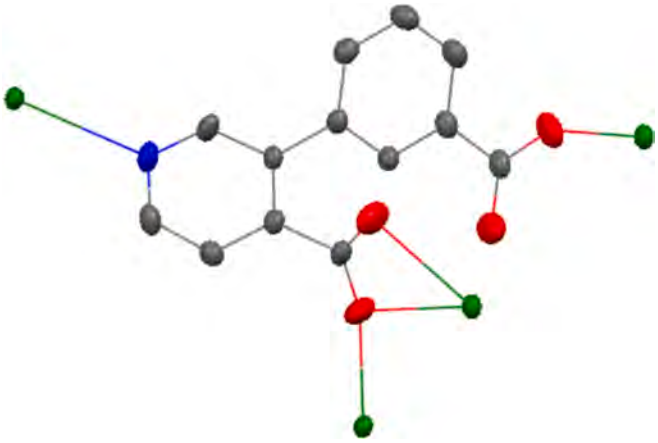

Fig. 6. The coordinated mode of COO^- groups.

(GGA) from the Perdew-Burke-Emzerhof (PBE) functional used to calculate the exchange-correlation function. The frontier molecular orbitals and electrostatic potential are shown in Fig. 8 and Fig. 9. The HOMO-LUMO orbital distribution of the Ba(II) coordination polymer shows that the HOMO orbitals (−0.25353 Ha (−6.899 eV)) are mainly located on the oxygen atoms coordinated to the barium ion, while the LUMO orbitals (−0.16381 Ha (−4.457 eV)) are primarily on the carbon chain structure. The calculated DFT energy gap is 0.08972 Ha (2.441 eV), indicating a moderate barrier for electronic transition. The electrostatic potential (ESP) of the Ba(II) coordination polymer reveals that regions with higher electrostatic potential are mainly concentrated in

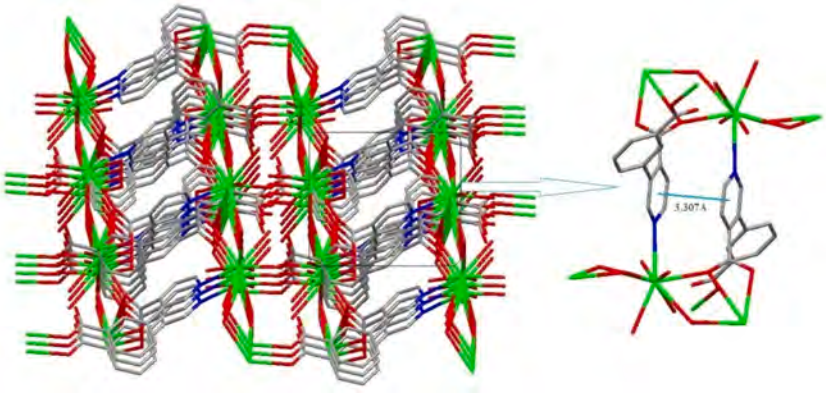

Fig. 7. The 3D network structure by π-π interactions.

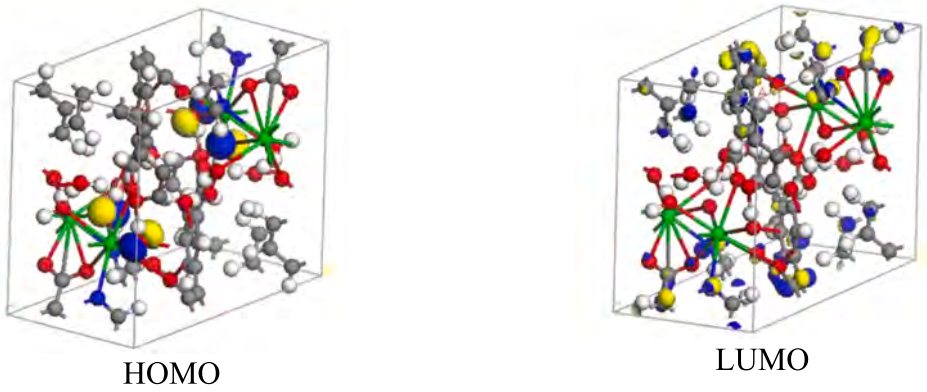

Fig. 8. The frontier molecular orbitals of the Ba(II) coordination polymer (isosurface = 0.8).

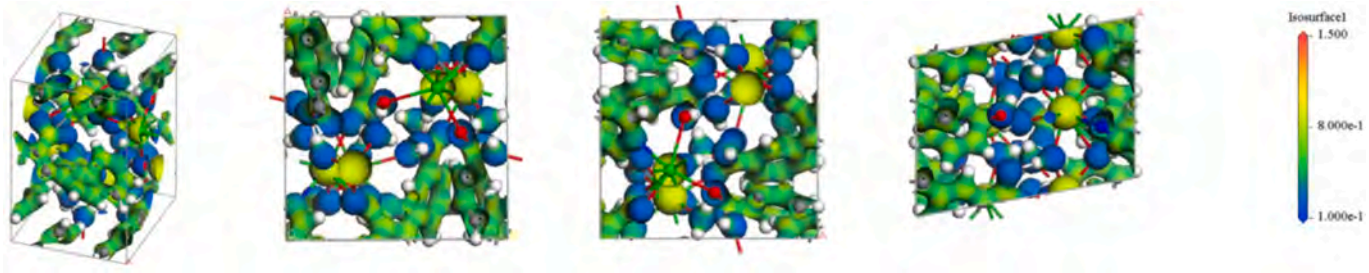

Fig. 9. Electrostatic potential of the Ba(II) coordination polymer (red for negative/electron-rich, blue for positive/electron-deficient). (For interpretation of the references to colour in this figure legend, the reader is referred to the web version of this article.)

the six-member carbon ring structures, while areas with lower potential are primarily found near oxygen and nitrogen atoms. This distribution indicates the electron-rich character of the heteroatom sites and the relative electron deficiency of the aromatic rings.

3.6. X-ray powder diffraction

X-ray powder diffraction (PXRD) analysis of the Ba(II) coordination polymer was conducted at room temperature ($5^\circ \leq 2\theta \leq 50^\circ$), and the resulting patterns are shown in Fig. 10. The experimental diffraction pattern (black) exhibits sharp, well-defined peaks, indicating the crystalline nature of the synthesized material. When compared with the simulated diffraction pattern (red) generated from single-crystal X-ray diffraction data, a clear, consistent overlap between the two sets of peaks is observed. This strong agreement between the measured and simulated PXRD patterns confirms that the bulk sample is phase-pure and structurally identical to the single-crystal model. The absence of additional peaks further indicates that no detectable impurities or secondary phases are present. Furthermore, the notable similarity between the simulated and experimental patterns highlights the high purity and structural stability of the Ba(II) coordination polymer under ambient conditions.

3.7. Catalytic performance

The catalytic activity of the Ba(II) coordination polymer was evaluated by the model oxidation of benzyl alcohol using molecular oxygen (O_2) as the sole oxidant [43–45]. The benzyl alcohol oxidation exhibited strong temperature dependence, as shown in Fig. 11. The catalytic activity of the blank (without catalyst) is very low (5.5% conversion) for the benzyl alcohol oxidation at 80 °C within 2 h under 5 bar of pressure O_2. The Ba(II) coordination polymer showed high benzyl alcohol

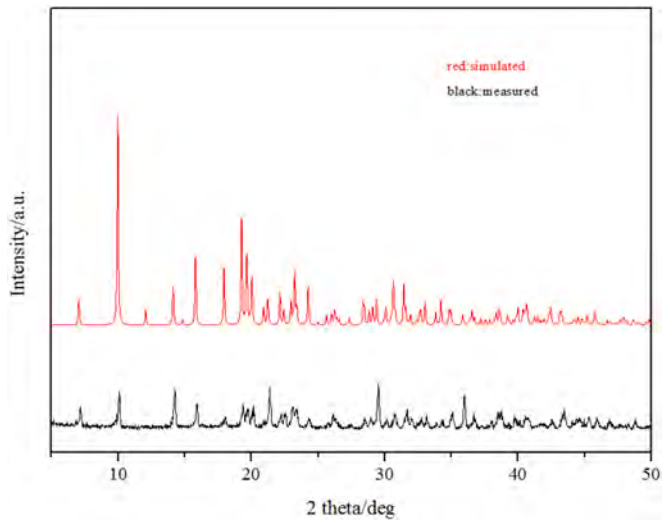

Fig. 10. Experimental (black) and simulated (red) PXRD patterns of the Ba(II) coordination polymer. (For interpretation of the references to colour in this figure legend, the reader is referred to the web version of this article.)

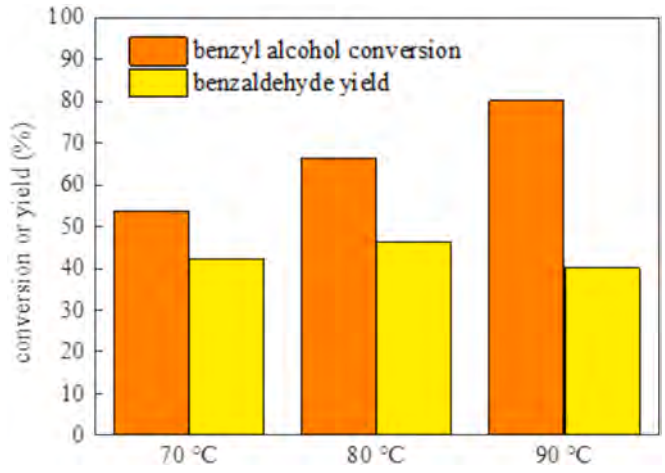

Fig. 11. Catalytic performance of Ba(II) coordination polymer for benzyl alcohol oxidation in THF (reaction conditions: benzyl alcohol (1.0 mmol), Ba(II) coordination polymer catalyst (0.02 g), THF (7 mL), 5 bar of O_2, 2 h).

conversion and benzaldehyde yield in the oxidation of benzyl alcohol. Benzoic acid was identified as the primary byproduct, along with trace amounts of benzyl benzoate. At 70 °C, the benzyl alcohol conversion and benzaldehyde yield were 53.6% and 42.3%, respectively. Increasing the temperature to 80 °C significantly improved both benzyl alcohol conversion and benzaldehyde yield, reaching 66.3% and 46.4%, respectively. At 90 °C, benzyl alcohol conversion reached 80.2%, while the benzaldehyde yield dropped to 37.5%, indicating substantial over-oxidation to benzoic acid at higher temperatures. These results show that 80 °C is optimal for both benzyl alcohol conversion and benzaldehyde selectivity. Compared with previously reported complexes, the Ba (II) coordination polymer exhibits superior catalytic performance in benzyl alcohol oxidation. The Ba(II) complex $[BaL_2Cl_2]$ (L = pyridine-2-carboxaldehyde-2-phenylacetic acid hydrazone) achieved only a 35.5% benzaldehyde yield with 67.0% conversion at 130 °C under 10 bar O_2 over 4 h [42]. Similarly, the Ni(II) complex $[Ni(L)_2(H_2O)_2]$ (L = 6-phenylpyridine-2-carboxylic acid) produced a 45.2% benzaldehyde yield with a 49.1% conversion at 90 °C under 7 bar O_2 within 2 h using THF as solvent [46]. The turnover frequencies (TOFs) are 7.2 h^{-1}, 1.8 h^{-1}, and 6.5 h^{-1} calculated based on the total metal (Ba or Ni) content in this work, Ref. [42] and Ref. [46], respectively. These comparisons clearly indicate that the Ba(II) coordination polymer exhibits significantly enhanced catalytic activity relative to the reference Ba(II) and Ni(II) complexes, highlighting its potential as an efficient catalyst for selective alcohol oxidation.

The stability of the Ba(II) coordination polymer was evaluated through recycling experiments. After each cycle, the Ba(II) coordination polymer catalyst was recovered by washing with anhydrous ethanol to remove organic residues and then dried at 80 °C for 12 h before reuse, and the recovery rate is 85%. The results from these catalytic recovery experiments are shown in Fig. 12. For the freshly prepared Ba(II) coordination polymer catalyst, the conversion of benzyl alcohol and the benzaldehyde yield were 66.3% and 46.4%, respectively. After four cycles, the conversion remained at 65.5%, and the yield was 45.9%. These results indicate that the Ba(II) coordination polymer catalyst did not undergo significant deactivation, demonstrating its good stability.

4. Conclusions

In summary, a novel three-dimensional Ba(II) coordination polymer, $[Ba(L)(H_2O)_3]_n$, was successfully synthesized using a one-pot method in an ethanol/H_2O/DMF mixture. A comprehensive characterization technique, including EA, IR, UV–vis spectroscopy, PXRD, and TGA, confirmed the polymer's composition and purity, while its single-crystal X-ray diffraction showed a nine-coordinated Ba(II) center within a monoclinic lattice. Density functional theory (DFT) calculations showed a HOMO–LUMO energy gap of 2.441 eV, and electrostatic potential analysis showed higher potential around the benzene rings and lower potential near the oxygen and nitrogen atoms. Notably, the Ba(II) coordination polymer demonstrated significant catalytic efficiency in benzyl alcohol oxidation, achieving 66.3% conversion and 46.4% benzaldehyde yield under mild conditions. These results establish $[Ba(L)(H_2O)_3]_n$ as a structurally stable and catalytically active material with potential uses in selective alcohol oxidation reactions. This work provides a theoretical basis for further synthesis of Ba(II) complexes and study of their catalytic activity.

CRediT authorship contribution statement

Tai Xi-Shi: Writing – original draft, Validation, Supervision, Resources, Methodology, Investigation, Data curation, Conceptualization. **Wang Li-Hua:** Writing – original draft, Validation, Resources, Methodology, Investigation. **Saud I. Al-Resayes:** Writing – review & editing, Supervision, Investigation, Conceptualization. **Mohammad Azam:**

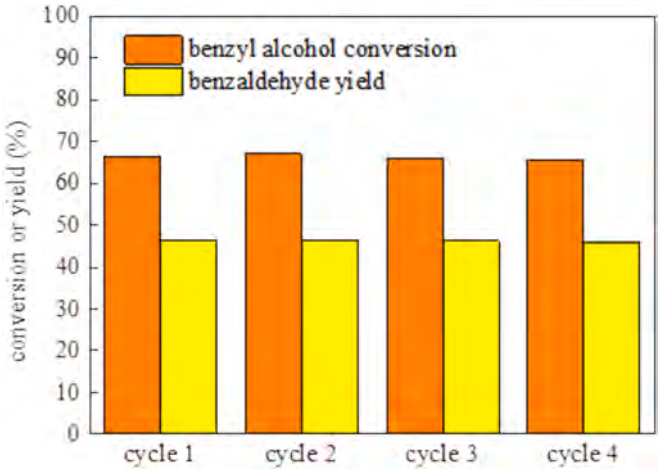

Fig. 12. Recyclability of the Ba(II) coordination polymer in benzyl alcohol oxidation (reaction conditions: 1 mmol benzyl alcohol, 7 mL THF, 0.02 g of Ba (II) coordination polymer, 80 °C, 5 bar of O_2, 2 h).

Writing – review & editing, Visualization, Supervision, Resources, Methodology, Investigation, Data curation, Conceptualization.

Declaration of competing interest

The authors declare that they have no known competing financial interests or personal relationships that could have appeared to influence the work reported in this paper.

Acknowledgments

This project was supported by National Natural Science Foundation of China (No. 21171132) and Science Foundation of Weiyuan Scholars Innovation Team. The authors acknowledge the financial support from the Ongoing Research Funding Program, (ORF-2025-147), King Saud University, Riyadh, Saudi Arabia.

Appendix A. Supplementary data

Supplementary data to this article can be found online at https://doi.org/10.1016/j.poly.2026.118009.

Data availability

Data will be made available on request.

References

[1] H. Furukawa, K.E. Cordova, M. O'Keeffe, O.M. Yaghi, The chemistry and applications of metal-organic frameworks, Science 341 (2013) 1230444.
[2] S. Du, H. Zhang, Metal-organic frameworks for photonics applications, in: B. Chen, G. Qian (Eds.), Structure and Bonding vol. 157, Springer Berlin Heidelberg, Berlin Heidelberg, 2014.
[3] Q. Zhao, X.H. Yi, C.C. Wang, P. Wang, W. Zheng, Photocatalytic Cr(VI) reduction over MIL-101(Fe)-NH2 immobilized on alumina substrate: from batch test to continuous operation, Chem. Eng. J. 429 (2022) 132497.
[4] C. Duan, Y. Yu, J. Xiao, Y. Li, P. Yang, F. Hu, H. Xi, Recent advancements in metal–organic frameworks for green applications, Green Energy Environ. 6 (2021) 33–49.
[5] H. Fu, C.C. Wang, W. Liu, MOFs for water purification, Chin. Chem. Lett. 33 (2022) 1647–1649.
[6] Y. Sun, Y. Liu, Design of metal-organic framework membranes towards ultimate gas separation, Green Chem. Eng. 2 (2021) 14–16.
[7] S. Yu, H. Pang, S. Huang, H. Tang, S. Wang, M. Qiu, Z. Chen, H. Yang, G. Song, D. Fu, B. Hu, X. Wang, Recent advances in metal-organic framework membranes for water treatment: a review, Sci. Total Environ. 800 (2021) 149662.
[8] A. Paul, L.M.D.R.S. Martins, A. Karmakar, M.L. Kuznetsov, A.A. Novikov, M.F.C. G. da Silva, A.J.L. Pombeiro, Environmentally benign benzyl alcohol oxidation and C-C coupling catalysed by amide functionalized 3D co(II) and Zn(II) metal organic frameworks, J. Catal. 385 (2020) 324–337.
[9] M.N. Khrizanforov, F.F. Naileva, K.A. Ivshin, A.A. Zagidullin, A.P. Samorodnova, P. V. Milyukova, R.P. Shekurov, A.I. Laskin, A.S. Novikov, V.A. Miluykov, Ugi's amine based coordination polymers as synergistic catalysts for the electrocatalytic reduction of carbon dioxide, Dalton Trans. 53 (2024) 17351–17360.
[10] A.N. Usoltsev, S.A. Adonin, P.A. Abramov, A.S. Novikov, V.R. Shayapov, P. E. Plyusnin, I.V. Korolkov, M.N. Sokolov, V.P. Fedin, 1D and 2D polybromotellurates (IV):structural studies and thermal stability, Eur. J. Inorg. Chem. 2018 (2018) 3264–3269.
[11] K. Biradha, A. Ramanan, J.J. Vittal, Coordination polymers versus metal−organic frameworks, Cryst. Growth Des. 9 (2009) 2969–2970.
[12] N. Yuan, Coordination polymers and clusters based on the versatile mercaptonicotinate ligands, Eur. J. Inorg. Chem. 43 (2019) 4607–4620.
[13] G. Guo, T. Wang, X. Ding, H. Wang, Q. Wu, Z. Zhang, S. Ding, S. Li, J. Li, Fluorescent lanthanide metal-organic framework for rapid and ultrasensitive detection of methcathinone in human urine, Talanta 249 (2022) 123663.
[14] S. Khan, M. Falahati, W.C. Cho, Y. Vahdani, R. Siddique, M. Sharifi, L. A. JaraghAlhadad, S. Haghighat, X. Zhang, T.L.M. ten Hagen, Core–shell inorganic NP@MOF nanostructures for targeted drug delivery and multimodal imaging guided combination tumor treatment, Adv. Colloid Interface Sci. 321 (2023) 103007.
[15] Z. Mehri Lighvan, S.R. Hosseini, S. Norouzbahari, B. Sadatnia, A. Ghadimi, Synthesis, characterization, and selective gas adsorption performance of hybrid NH_2-MIL-101(Fe)/ZIF-8 metal organic framework (MOF), Fuel 351 (2023) 128991.
[16] A. de Oliveira, S. Grigoletto, L. Fernanda Menezes Alves Vieira, S. Júlia Fernandes Amorim, H. Avelino De Abreu, Unveiling the adsorption mechanism of arsenic species in the MOF-74 through an in-silico approach targeting the development of adsorbents for polluted water treatment, Chem. Phys. Lett. 831 (2023) 140841.
[17] C. Zhang, K. Lu, L. Li, W. Lei, M. Xia, F. Wang, A water-stabilized Tb-MOF can be used as a sensitive and selective fluorescence sensor for the detection of oxytetracycline hydrochloride, Spectrochim. Acta Part A-Mol. Biomol. Spectrosc. 304 (2024) 123379.
[18] W. Chen, L. Du, C. Wu, Chapter 7-hydrothermal synthesis of MOFs, in: M. Mozafari (Ed.), Metal-Organic Frameworks for Biomedical Applications, Woodhead Publishing, 2020, pp. 141–157. ISBN 978-0-12-816984-1.
[19] A. Ghoorchian, A. Afkhami, T. Madrakian, M. Ahmadi, Chapter 9-electrochemical synthesis of MOFs, in: M. Mozafari (Ed.), Metal-Organic Frameworks for Biomedical Applications, Woodhead Publishing, 2020, pp. 177–195. ISBN 978-0-12-816984-1.
[20] S.H. Jhung, J.H. Lee, P.M. Forster, G. F'erey, A.K. Cheetham, J.S. Chang, Microwave synthesis of hybrid inorganic-organic porous materials: phase-selective and rapid crystallization, Chemistry 12 (2006) 7899–7905.
[21] R. Akhavan-Sigari, M. Zeraati, M. Moghaddam-Manesh, P. Kazemzadeh, S. Hosseinzadegan, N.P.S. Chauhan, G. Sargazi, Porous Cu-MOF nanostructures with anticancer properties prepared by a controllable ultrasound-assisted reverse micelle synthesis of Cu-MOF, BMC Chem. 16 (2022) 10.
[22] X. Li, Z. Wu, X. Tao, R. Li, D. Tian, X. Liu, Gentle one-step Co-precipitation to synthesize bimetallic CoCu-MOF immobilized laccase for boosting enzyme stability and Congo red removal, J. Hazard. Mater. 438 (2022) 129525.
[23] McGuire, C.V., Forgan, R.S. In: Second ed, in: S. Kaskel (Ed.), The Surface Chemistry of Metaleorganic Frameworks, vol. 51, WILEY-VCH, Weinheim, 2015.
[24] F. Moghzi, J. Soleimannejad, J. Janczak, Dual-emitting barium based metal-organic nanosheets as a potential sensor for temperature and anthrax biomarkers, Nanotechnology 31 (2020) 245706.
[25] S. Zhang, X.N. Qu, G. Xie, Q. Wei, S.P. Chen, Syntheses, structural analyses and luminescent property of four alkaline-earth coordination polymers, J. Solid State Chem. 210 (2014) 36–44.
[26] G. Wu, F.J. Yin, H.H. Li, L. Guo, Syntheses, structure and properties of barium (II) complex with 2,3-pyrazinedicarboxylic acid, J. Chem. Crystallogr. 42 (2012) 680–684.
[27] Drzewiecka-Antonik, A., Koziol, A.E., Rejmak, P., Lawniczak-Jablonska, K., Nittler, L., Lis, T. Novel Ba(II) and Pb(II) coordination polymers based on citric acid: synthesis, crystal structure and DFT studies. Polyhedron, 2017, l 132, 1–11.
[28] L. Zuo, J.H. Feng, L. Guo, H.H. Li, G. Wu, Synthesis, structure, luminescence, and thermal stability properties of 3,4-pyridinedicarboxylic acid barium complex, Chinese J. Inorg. Chem. 29 (2013) 1979–1984.
[29] Q.G. Meng, M.H. Zhang, L.L. Zhang, R.M. Wang, D.F. Sun, A 3D Ba(II) inorganic-organic hybrid framework based on 1,3,5-benzenetricarboxylic acid ligand: synthesis and characterization, Chin. J. Struct. Chem. 33 (2014) 1560–1565.
[30] J. Cai, J.Y. Lu, Q.Y. Chen, L.L. Qu, Y.Q. Lu, G.F. Gao, Eu-based MOF/graphene oxide composite: a novel photocatalyst for the oxidation of benzyl alcohol using water as oxygen source, New J. Chem. 41 (2017) 3882–3886.
[31] T.H. Tan, J. Scott, Y.H. Ng, R.A. Taylor, K.F. Aguey-zinsou, R. Amal, C–C cleavage by Au/TiO_2 during ethanol oxidation: understanding bandgap photoexcitation and plasmonically mediated charge transfer via quantitative in situ drifts, ACS Catal. 6 (2016) 8021–8029.
[32] M. Aliniya, R. Bikas, N. Heydari, M.S. Krawczyk, T. Lis, Sci. Rep. volume 15 (2025) 23027.
[33] X.S. Tai, L.H. Wang, S.I. Al-Resayes, M. Azam, Synthesis, structural characterization, Hirschfeld surface analysis, and catalytic application of a new Cd (II) complex bearing 1H-pyrazolo[3,4-b] pyridine-3-amine and pyridine carboxylic acid, Polyhedron 279 (2025) 117647.
[34] L.H. Wang, X.S. Tai, M. Azam, B.L. Sui, A.L. Wang, Synthesis, structural characterization, and Hirschfeld surface analysis of a novel Mn(II) complex based on N-acetyl-L-phenylalanine ligand and its evaluation as a cytotoxic agent, Polyhedron 279 (2025) 117659.
[35] X.S. Tai, X.J. Zhou, L.L. Liu, Synthesis, crystal structure and antitumor activity of a Na(I) coordination polymer based on 2-propyl-4,5-imidazoledicarboxylic acid and 1,10-phenanthroline ligands, Chinese J. Struct. Chem. 38 (2019) 1079–1085.
[36] Y. Liu, X. Tang, X.H. Yan, L.H. Wang, X.S. Tai, M. Azam, D.Q. Zhao, The synthesis, structural characterization, and DFT calculation of a new binuclear Gd (III) complex with 4-aacetylphenoxyacetic acid and 1,10-phenanthroline ligands and its roles in catalytic activity, Molecules 29 (2024) 3039.
[37] S.H. Cao, X.S. Tai, K.X. Li, A.L. Zhang, P.J. Ma, G.Q. Sui, L.S. Zhang, X.H. Tian, A. L. Wang, M. Azam, Two novel homo/hetero polynuclear complexes for DNA binding, molecular docking, and anti-cancer activity, J. Mol. Struct. 1325 (2025) 141040.
[38] G.M. Sheldrick, SHELXT-integrated space-group and crystal-structure determination, Acta Crystallogr. A71 (2015) 3–8.
[39] G.M. Sheldrick, Crystal structure refinement with SHELXL, Acta Crystallogr. C71 (2015) 3–8.
[40] Nakamoto K., Infrared and Ramen Spectra of Inorganic and Coordination Compounds, 3rd ed.; Wiley: New York, NY, USA, 1978; Volume 1, pp. 359–368.
[41] L. Zuo, J.H. Feng, L. Guo, H.H. Li, G. Wu, Synthesis, structure, luminescent, and thermal stable properties of 3,4-pyridinedicarboxylic acid barium complex, Chinese J. Inorg. Chem. 29 (2013) 1979–1984.
[42] L.H. Wang, X.S. Tai, L.L. Liu, P.F. Li, Synthesis, crystal structure, and catalytic activity of a novel Ba(II) complex with pyridine-2-carboxaldehyde-2-phenylacetic acid hydrazone ligand, Crystals 7 (2017) 305–311.
[43] L.L. Liu, X.J. Zhou, L. Liu, S. Jiang, Y.J. Li, L.X. Guo, S.J. Yan, X.S. Tai, Heterogeneous bimetallic Cu–Ni nanoparticle-supported catalysts in the selective oxidation of benzyl alcohol to benzaldehyde, Catalysts 9 (2019) 538–555.
[44] L. Liu, X. Zhou, C. Xin, B. Zhang, G. Zhang, S. Li, L. Liu, X. Tai, Efficient oxidation of benzyl alcohol into benzaldehyde catalyzed by graphene oxide and reduced

graphene oxide supported bimetallic Au–Sn catalysts, RSC Adv. 13 (2023) 23648–23658.
[45] Y. Liu, L. Li, L. Liu, L. Wang, M. Zang, X. Zhou, M. Azam, X. Tai, Bimetallic Au–Ru nanoparticles supported on zeolitic imidazolate framework-67 as highly efficient catalysts for the selective oxidation of benzyl alcohol, Sci. Rep. 15 (2025) 12145–12157.
[46] L.H. Wang, F.Y. Kong, X.S. Tai, Synthesis, structural characterization of a new Ni (II) complex and its catalytic activity for oxidation of benzyl alcohol, Bull. Chem. React. Eng. Catal. 17 (2022) 375–382.